

The crystal structure and thermal expansion of Mo_5SiB_2

C.J. Rawn*, J.H. Schneibel, C.M. Hoffmann¹, C.R. Hubbard

Metals and Ceramics Division, Oak Ridge National Laboratory, Oak Ridge, TN 37831, USA

Received 24 April 2000; accepted 24 August 2000

Abstract

Mo_5SiB_2 (T2), synthesized with ^{11}B , was studied using high temperature neutron powder diffraction. This ternary compound crystallizes with a tetragonal unit cell, space group $I4/mcm$, with room temperature lattice parameters $a=6.0272(3)$ and $c=11.0671(7)$ Å. The structural refinement reveals that B substitutes for a minor amount of Si for a formula of $\text{Mo}_5\text{Si}_{0.89}\text{B}_{2.11}$. The refined lattice parameters studied as a function of temperature give average thermal expansion coefficients along the a and c-axes, $(7.9\pm 0.1)\times 10^{-6}$ K⁻¹ and $(7.5\pm 0.2)\times 10^{-6}$ K⁻¹, respectively. The thermal expansion of Mo_5SiB_2 is, therefore, nearly isotropic. A more detailed evaluation shows that the thermal expansion coefficient, as well as the thermal expansion anisotropy, vary with temperature. Published by Elsevier Science Ltd. All rights reserved.

Keywords: A. Molybdenum silicides; B. Thermal properties; B. Crystallography

1. Introduction

High temperature silicides are an important class of materials, and were the subject of a recent symposium [1]. Some silicides, in particular MoSi_2 , exhibit excellent high temperature oxidation resistance. However, their mechanical properties are often inadequate. MoSi_2 , for example, exhibits a low room temperature fracture toughness on the order of 3 MPa m^{1/2} [2,3]. Its creep strength is low and needs to be improved, for example, by fabricating composites containing as much as 50 vol.% Si_3N_4 . In the hope of finding better combinations of properties, alternative molybdenum silicide compounds have been explored in recent years. Of particular interest are the compounds Mo_3Si , Mo_5Si_3 (T1), and Mo_5SiB_2 (T2). Nowotny et al. [4] identified the T2 phase in a 1873 K isothermal section of the ternary Mo–Si–B phase diagram and also mentioned the possibility of improved oxidation resistance due to the formation of borosilicates. A slightly revised version of Nowotny's 1873 K isothermal phase diagram, which has been published by Nunes, Sakidja, and Perepezko [5], is shown in Fig. 1. Berczik [6,7] focused on alloys containing α -Mo,

Mo_3Si , and T2. In those alloys, the α -Mo provides toughening and ductility. Berczik's alloys are essentially Mo alloys containing intermetallic particles and can be considered as α -Mo metal matrix composites containing intermetallic particles. Schneibel et al. [8], on the other hand, investigated alloys with α -Mo volume fractions of 50% or less, which consisted of toughening α -Mo particles embedded in a $\text{Mo}_3\text{Si}/\text{T2}$ matrix. Meyer et al. [9] focused on alloys containing only brittle phases, namely, Mo_3Si , T1, and T2. They found good oxidation and creep resistance. Recently, Chu et al. [10] and Fu et al. [11] investigated the phase Mo_5Si_3 in more detail. Chu et al. [10] grew single crystals of Mo_5Si_3 and determined their coefficients of thermal expansion (CTE), which exhibited a high anisotropy, namely, $\alpha_c/\alpha_a=2.2$. Using resonant ultrasound spectroscopy, they also determined the elastic constants. Fu et al. [11] carried out first-principles local-density-functional calculations and found excellent agreement with Chu et al.'s [10] elastic constants. They attributed the high CTE anisotropy to the strong bonding within the (001) planes and the high anharmonicity in the [001] direction. The high thermal expansion anisotropy and associated microcracking are the reason why arc-cast buttons of Mo_5Si_3 disintegrate into powder on sectioning [12]. Similarly, Thom et al. [13], report microcracking in Ti_5Si_3 , which exhibits a slightly higher CTE anisotropy than T1 ($\alpha_c/\alpha_a=2.3$).

* Corresponding author.

E-mail address: rawncj@ornl.gov (C.J. Rawn).

¹ Present address: Philips Analytical, Natick, MA 01760, USA.

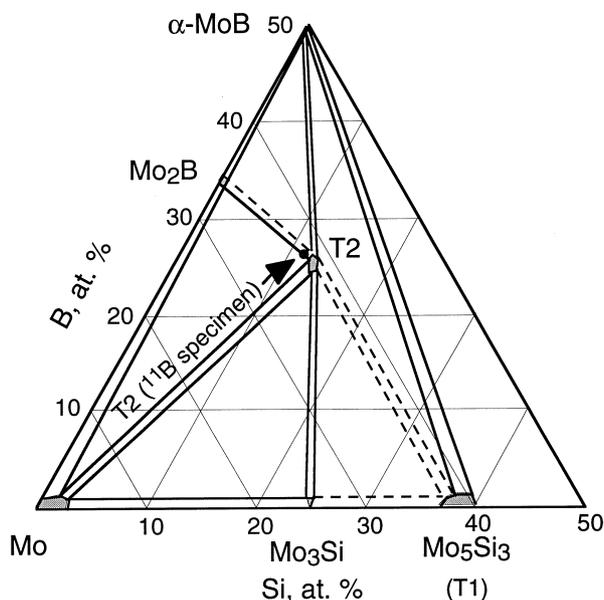


Fig. 1. Portion of the Mo-Si-B phase diagram as reported by Nunes et al. [5]. $T = 1873$ K.

The thermal expansion coefficients of the T2 phase have so far not been examined. There are several reasons for this. First, it is difficult to prepare single phase T2 by arc-melting, since the solidification involves the primary precipitation of MoB [5]. Even after annealing for 150 h at 1873 K, arc-melted alloys with the nominal T2 composition, Mo_5SiB_2 , contain MoB and Mo_5Si_3 [14]. In compositions close to T2, second phases such as α -Mo, Mo_3Si , and Mo_2B can be found. Because of the complicated solidification sequence, it is difficult to grow single crystals of the T2 phase. This means that conventional thermal expansion measurements by dilatometry would be difficult to carry out and that powder diffraction lattice parameter measurements as a function of temperature are preferable. In the present work we prepared nominally single phase T2 by arc-casting followed by annealing at high temperatures. The CTE was determined by neutron powder diffraction at temperatures up to 1652 K in vacuum. In addition, the details of the T2 crystal structure, as well as its chemical composition, were determined.

2. Experimental procedures

2.1. Synthesis and characterization

Two 19 g buttons with the nominal composition Mo_5SiB_2 were arc-cast from high-purity elemental materials in argon on a water-cooled copper hearth. Because of small weight losses during melting and casting (typically 1 wt.%), the actual compositions will deviate from the nominal compositions. As compared to arc-cast Mo_5Si_3 , only minor microcracking was observed, suggesting a

low CTE anisotropy. One button was cast with boron enriched in ^{11}B (98.68 at.%, Eagle Picher). This button was used for the neutron diffraction experiments because ^{10}B has a large absorption cross section, σ_a , [$\sigma_a = 3835(9)$ barn for ^{10}B as compared to $\sigma_a = 0.0055(33)$ barn for ^{11}B]. The bound coherent scattering lengths (b_c) are 6.715(20), 4.1491(10), $-0.1-1.066(3)i$, and 6.65(4) fm for Mo, Si, ^{10}B , and ^{11}B , respectively [15]. The other button was cast with B with the naturally occurring isotopic ratio, which corresponds to approximately 20 at.% ^{10}B .

The ^{11}B button was annealed by induction heating in He for 12 h at 2270 K followed by 0.5 h at 1670 K. Using an Al_2O_3 mortar and pestle it was subsequently ground into < 45 μm powder for the neutron diffraction. The other button was annealed in He for 0.5 h at 2370 K followed by 0.5 h at 1670 K. It was sectioned, polished, etched with Murakami's etch, and examined in an electron microprobe equipped with a wavelength-dispersive spectrometer (WDS). Its Vickers hardness number was determined with a load of 500 g and a dwell time of 15 s.

2.2. Neutron powder diffraction

Neutron diffraction measurements were conducted at the high flux isotope reactor (HFIR) on the HB-4 high-resolution neutron powder diffractometer [16]. HB-4 is equipped with a Ge(115) monochromator and 32 equally spaced ^3He detectors. The wavelength was determined to be 1.50053 Å using silicon powder (NIST SRM 640b). The powder sample was contained in a cylindrical vanadium can suspended in an ILL (Institute Laue Langevin) vacuum furnace equipped with Nb heating elements. The furnace control temperature was checked up to 1373 K against a second, independent, type K thermocouple that was inserted into a V can filled with Al_2O_3 powder. A correction curve, generated from the difference between the control temperature and the temperature of the independent thermocouple, was applied to obtain a set of corrected temperatures. Data were collected at 300, 620, 890, 1179, 1468 and 1652 K using constant monitor counts with a step size of 0.05° 2θ between 11 and 135° 2θ so that each run was approximately 13 h. During the 1652 K data collection, the bolt holding the V can broke and the sample fell off, rendering only data below 98° 2θ useable.

For the Rietveld refinements, the General Structure Analysis System (GSAS) was used [17]. Preliminary refinements with the B present as 100% ^{11}B , on the room temperature data set, resulted in several negative atomic displacement parameters (ADP). This underestimation of the Debye-Waller factors could possibly be due to attenuation of the neutron beam through the sample. To investigate this we measured the transmission of the neutron beam through both the Mo_5SiB_2 and the starting ^{11}B using the procedure outlined by

Hewat [18]. In both cases the beam was attenuated by the sample, suggesting that ^{10}B , which has an absorption cross section (σ_a) seven orders of magnitude higher than that of ^{11}B , is an impurity in the ^{11}B used for preparing the specimens. With the above justification the Debye–Scherrer absorption correction was taken into account. Preliminary refinements suggested that a minor amount of B was located on the Si site. In order to accommodate this site sharing in the refinement all sites were constrained to 100% occupation by one or two different atoms or isotopes so that all the B on the Si site was ^{11}B and that the B site was 98.7% filled with ^{11}B and 1.3% filled with ^{10}B . These assumptions are probably slightly different from the actual circumstances where a minor amount of ^{10}B could be present in the Si site and/or vacancies could be present on either of the shared sites.

3. Results and discussion

Fig. 2 shows a backscattered scanning electron microscope (BS SEM) micrograph of the annealed, polished and etched specimen made with the naturally occurring isotopic ratio of B. The major phase is T2. As expected from Nunes et al.'s [5] work, the alloy con-

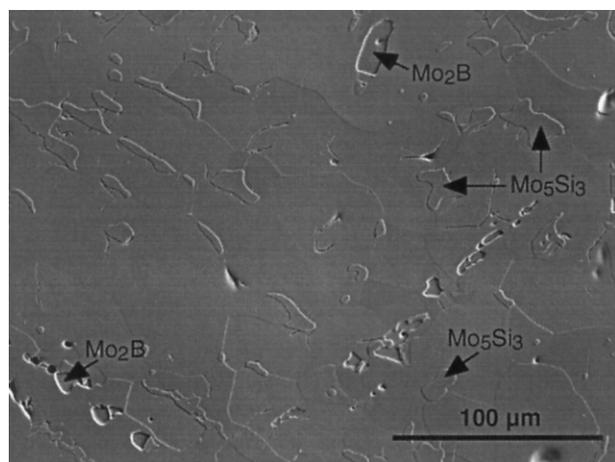


Fig. 2. Backscattered scanning electron microscope (BS SEM) micrograph of the annealed, polished and etched sample of T2 made with

tained secondary phases. Sakidja et al. [14] found MoB, Mo_3Si , and Mo_5Si_3 as second phases in an arc-melted alloy with the nominal composition Mo_5SiB_2 annealed for 150 h at 1870 K. Presumably because of a slightly different actual composition, a higher annealing temperature, and incomplete equilibration, our button contained Mo_5Si_3 as the largest volume fraction of impurity phase and Mo_2B with a lower volume fraction than that of Mo_5Si_3 . Mo_2B is easily recognized because it is preferentially etched. The Vickers hardness number of the T2 phase, determined from 10 impressions, was 1684 ± 39 . This corresponds to a hardness, i.e. load divided by projected area, of (17.8 ± 0.4) GPa. Consistent with the brittle nature of T2, cracks originated at the indent corners.

The starting structural model for the refinement was based on the crystal structure reported by Aronsson [19]. Our results confirm the structure (tetragonal, space group I4/mcm), and Table 1 gives the refined fractional coordinates, site occupancies, and the atomic displacement parameters (ADPs) at room temperature. Numbers in parentheses are estimated standard deviations (esd's) in the last significant figure of the refined parameter. Fig. 3 is the structure drawn from the results given in Table 1. Note that all the atoms are on special positions and that the site symmetry restricts the components of the thermal-motion tensors (e.g. for the Si atom $(0,0,1/4)$ $U_{11} = U_{22}$ and $U_{12} = U_{13} = U_{23} = 0$) [20]. Aronsson [19] reports a range of lattice parameters for the T2 phase. Based on the range of lattice parameters and chemical analysis that indicated that the Si/B ratio did not exceed 0.5, Aronsson [19] suggested a homogeneity range that could be deficient in Si and at the same time have excess B. Our findings of B substituting for a minor amount of Si for a formula of $\text{Mo}_5\text{Si}_{0.89}\text{B}_{2.11}$ (see Rietveld analysis) agrees well with Aronsson's [19] results. This result suggests also that the composition of T2 can be lower in Si and higher in B than that in the 1873 K isothermal phase diagram.

SEM observations of the ground button enriched with ^{11}B showed small Al_2O_3 particles on the T2 powder particles. Since the grinding was performed with an Al_2O_3 mortar and pestle, and the T2 phase is hard, it is not surprising to find minor amounts of Al_2O_3 . To

Table 1
Refined fractional coordinates, site occupancies, and ADPs for the Mo_5SiB_2 phase at room temperature

Atom	Site	x	y	z	Occupancy	$U_{\text{anisotropic}} (10^{-2} \text{ \AA}^2)$			
						U_{11}	U_{33}	U_{12}	U_{13}
Si/ ^{11}B	4a	0	0	1/4	0.89/0.11(3) ^a	0.5(2)	0.4(2)	–	–
$^{11}\text{B}/^{10}\text{B}$	8h	0.3784(2)	$x + 1/2$	0	0.987/0.013	0.22(5)	0.25(8)	0.09(6)	–
Mo_{I}	4c	0	0	0	1.0	0.17(7)	0.3(1)	–	–
Mo_{II}	16l	0.1641(1)	$x + 1/2$	0.1398(1)	1.0	0.23(3)	0.52(5)	0.00(4)	–0.05(3)

^a esd's reported in 1 σ .

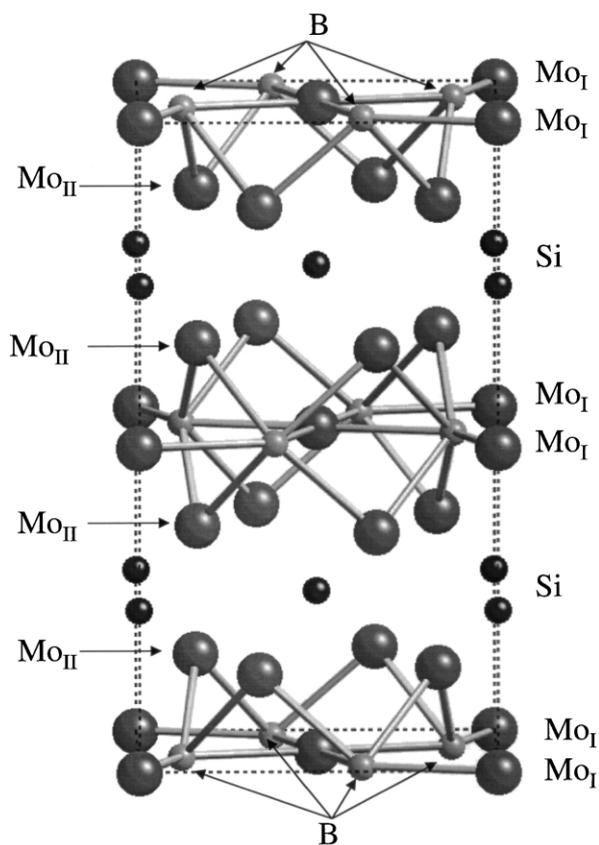


Fig. 3. Structure of Mo_5SiB_2 drawn from the atomic coordinates given in Table 1.

account for diffraction maxima not belonging to the T2 phase, Mo, Mo_3Si , and Al_2O_3 (3, 5, and 1 wt.%, respectively) had to be introduced to model the neutron powder diffraction pattern. This indicates that the actual composition of the ^{11}B specimen was slightly different from that of the specimen containing the naturally occurring boron (although the nominal compositions were identical). Reference to Fig. 1 shows that a small change in composition can easily move the phase assemblage into the Mo– Mo_3Si –T2 equilibrium triangle. Since no other phases were found it appears that the ^{11}B specimen reached equilibrium during its anneal (which was at a lower temperature, but much longer than that of the specimen with naturally occurring boron). The Al_2O_3 was used as an additional check for the thermal expansion measurements.

The profile agreement factors for the Rietveld refinements at the various temperatures are given in Table 2, where wR_p is the weighted pattern R index and χ , the goodness of fit, is the ratio of wR_p to R_{exp} , the minimum possible weighted residual for the powder pattern. A χ value between 1.0 and 1.5 indicates a satisfactory fit. All the χ 's in Table 2 are in this range with the exception of the 300 K and the 1652 K refinements, which have a lower and higher R_{exp} , respectively, than calculated for the other powder patterns. Fig. 4 shows the comparison

Table 2
Profile agreement factors for the Rietveld refinements

Temperature (K)	R_{exp} (%)	wR_p (%)	χ	Number of variables
300	4.71	7.62	1.62	45
620	6.04	8.26	1.37	45
890	6.46	8.35	1.29	45
1179	5.40	7.39	1.37	45
1468	6.21	8.07	1.30	45
1652 ^a	7.41	13.99	1.89	45

^a Data refined only up to $98^\circ 2\theta$.

of the observed neutron powder diffraction data with the calculated pattern for the room temperature data set.

Table 3 gives the anisotropic ADPs at the various temperatures for Mo_5SiB_2 . U_{eq} is defined as $1/3$ the trace of the diagonalized matrix. The Debye temperature, Θ_D , was estimated to be 467 K using the room temperature ADPs (U_{eq}) given in Table 3 [21,22]. This is approximately 30% less than the first principles calculated value of approximately 600 K [23]. An underestimation of Θ_D indicates that the U_{eq} values are slightly overestimated. This overestimation could be directly related to the absorption correction to account for a small amount of ^{10}B . The ADPs that represent the magnitude of vibration (i.e. U_{ii}) show an abrupt increase at 1652 K.

Table 4 compares the bond lengths for the various temperatures for Mo_5SiB_2 . The bond lengths reported by Aronsson [19] are also included for comparison and agree well with the bond lengths determined from the Rietveld refinement of the 300 K data. In some cases the bond lengths increase linearly with temperature (e.g. the Si– Mo_1 bond length has a correlation factor of 0.995 for a straight line fit) and in some cases there is an abrupt increase at 1652 K (e.g. the B–B bond length has a correlation factor of 0.912 when the bond length at 1652 K is included, and excluding this bond length results in a correlation factor of 0.992). The abrupt increase in the ADPs and $^{11}\text{B}/\text{Si}$ ratio at 1652 K and the discontinuities of some of the bond lengths as a function of temperature could indicate a phase transition. However, comparing the neutron powder diffraction pattern collected at 300 K to the pattern collected at 1652 K, the patterns are essentially identical except for the shifting of the peaks due to thermal expansion, and linear fits to a and c versus temperature have correlation factors close to one. These results indicate that the abrupt changes observed could result from the loss of Si in the structure rather than a phase transformation. Note that the Si– Mo_1 bonds, which increase linearly in length with temperature over the entire temperature range, lie along the z axis while the B–B bonds, which increase linearly with temperature up to 1468 K and then change abruptly between 1468 and 1652 K, lie entirely in the xy plane.

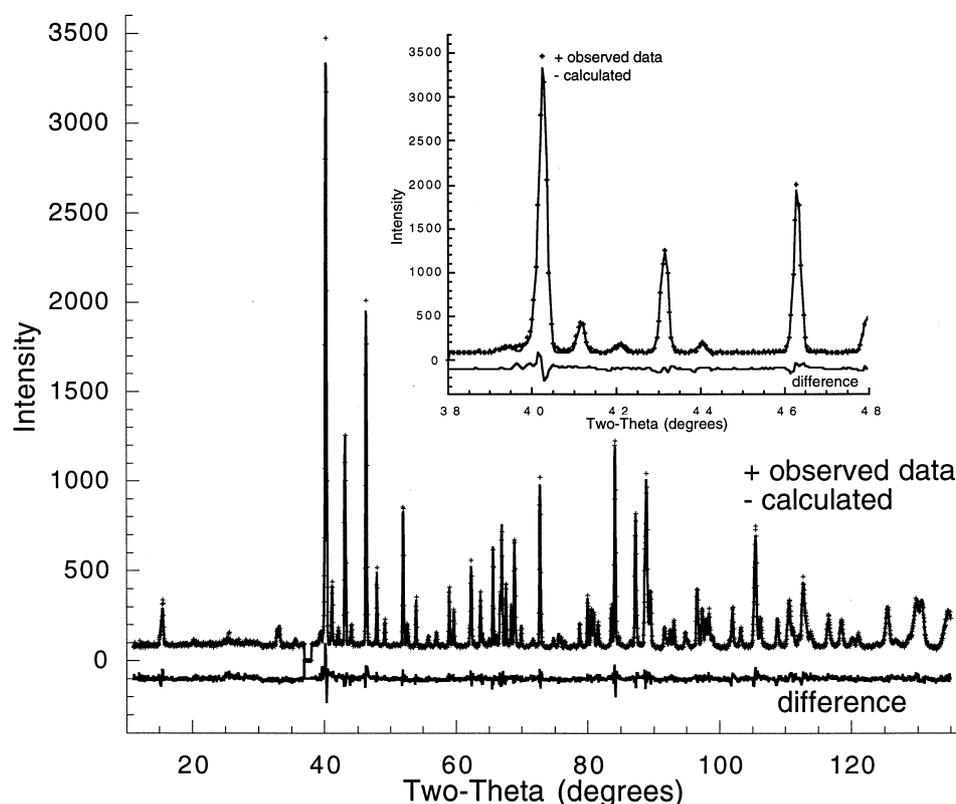


Fig. 4. Comparison of the observed neutron powder diffraction data (+) with the calculated pattern (solid line) and the difference pattern for the room temperature data set ($\lambda = 1.500 \text{ \AA}$). The data between 37 and $38^\circ 2\theta$ has been excluded due to the presence of the Nb (110) reflection from the heating elements in the ILL furnace.

Table 3

Temperature dependence of atomic displacement parameters in units of 10^{-2} \AA^2 for Mo_5SiB_2

Atom		Temperature (K)					
		300	620	890	1179	1468	1652
Si	U_{eq}	0.44	0.79	0.87	1.54	1.27	5.27
	$U_{11} = U_{22}$	0.5(2) ^a	0.9(2)	0.8(2)	1.4(2)	1.2(2)	4.3(6)
	U_{33}	0.4(2)	0.6(3)	0.9(3)	1.7(3)	1.5(3)	7(1)
B	U_{eq}	0.23	0.55	0.90	1.21	1.64	4.60
	$U_{11} = U_{22}$	0.22(5)	0.52(5)	0.85(6)	1.18(6)	1.61(7)	5.5(2)
	U_{33}	0.25(8)	0.6(1)	1.0(1)	1.3(1)	1.7(1)	2.8(3)
	U_{12}	0.09(6)	0.14(8)	0.25(9)	0.36(9)	0.4(1)	0.6(4)
Mo_I	U_{eq}	0.21	0.45	0.65	0.85	1.17	3.44
	$U_{11} = U_{22}$	0.17(2)	0.34(8)	0.38(9)	0.62(9)	0.9(1)	3.0(3)
	U_{33}	0.3(1)	0.6(2)	1.2(2)	1.3(2)	1.8(2)	4.3(5)
Mo_{II}	U_{eq}	0.33	0.61	0.89	1.20	1.53	4.56
	$U_{11} = U_{22}$	0.23(3)	0.57(4)	0.89(4)	1.23(4)	1.56(5)	4.4(1)
	U_{33}	0.52(5)	0.68(6)	0.91(7)	1.15(7)	1.46(8)	5.0(3)
	U_{12}	0.00(4)	0.12(5)	0.07(5)	0.24(5)	0.31(6)	0.4(2)
	$U_{13} = U_{23}$	-0.05(3)	-0.04(3)	0.01(4)	-0.12(4)	-0.13(4)	-0.9(1)

^a esd's are reported as 1σ .

Table 5 gives the refined lattice parameters, a and c , the unit cell volume, and the cube root of the unit cell volume, as a function of temperature. These lattice parameter values are slightly less than those determined

by Kramer [24]. The differences most likely arise due to a compositional difference. Straight line fits of the two data sets reveal the slopes to be within 5% of each other. Fig. 5 plots $\Delta L/L_0$ versus temperature where L_0

Table 4
Bond lengths in Å as function of temperature

	Aronsson [19]	300 K ^a	620 K	890 K	1179 K	1468 K	1652 K
Si–Mo _I ^b	2.77(2)	2.76676(5)	2.77244(6)	2.77754(6)	2.78382(6)	2.79107(7)	2.7969(2)
Si–Mo _{II}	2.56(8)	2.5619(6)	2.5677(7)	2.5723(7)	2.5773(7)	2.5848(8)	2.587(2)
B–B	2.13	2.072(3)	2.086(4)	2.097(4)	2.107(4)	2.113(4)	2.16(1)
B–Mo _I	2.38(2)	2.3957(7)	2.3998(8)	2.4029(9)	2.4072(8)	2.413(1)	2.409(3)
B–Mo _{II}	2.34(4)	2.329(1)	2.337(1)	2.343(2)	2.351(2)	2.355(2)	2.372(4)
	2.36(6)	2.395(2)	2.398(2)	2.403(2)	2.407(2)	2.413(2)	2.411(6)
Mo _I –Mo _{II}	2.72(8)	2.7336(7)	2.7408(7)	2.7479(8)	2.7549(8)	2.7611(9)	2.772(2)
Mo _{II} –Mo _{II}	2.82	2.797(2)	2.803(2)	2.804(3)	2.811(2)	2.816(3)	2.813(7)
	2.85	2.844(2)	2.849(2)	2.853(3)	2.857(3)	2.868(3)	2.863(6)
	3.07	3.095(2)	3.104(2)	3.114(3)	3.124(3)	3.129(3)	3.149(6)
	3.17(2)	3.140(2)	3.144(2)	3.145(2)	3.150(2)	3.160(3)	3.153(6)
	3.18(4)	3.1866(4)	3.1949(5)	3.2022(6)	3.2093(6)	3.2175(6)	3.225(2)

^a esd's for the data reported in this study are 1σ .

^b $1/4c$ due to fixed positions.

Table 5
T2 lattice parameters as a function of temperature

Temperature (K)	a (Å)	c (Å)	Volume (Å ³)	Volume $1/3$ (Å)
300	6.0272(3) ^a	11.0671(7)	402.35(6)	7.3825(4)
620	6.0422(4)	11.0898(7)	404.87(7)	7.3979(4)
890	6.0542(4)	11.1102(8)	407.22(8)	7.4121(5)
1179	6.0680(4)	11.1353(7)	410.01(7)	7.4290(4)
1468	6.0826(4)	11.1643(8)	413.06(8)	7.4474(5)
1652	6.0938(9)	11.188(2)	415.4(2)	7.462(1)

^a esd's reported in 3σ .

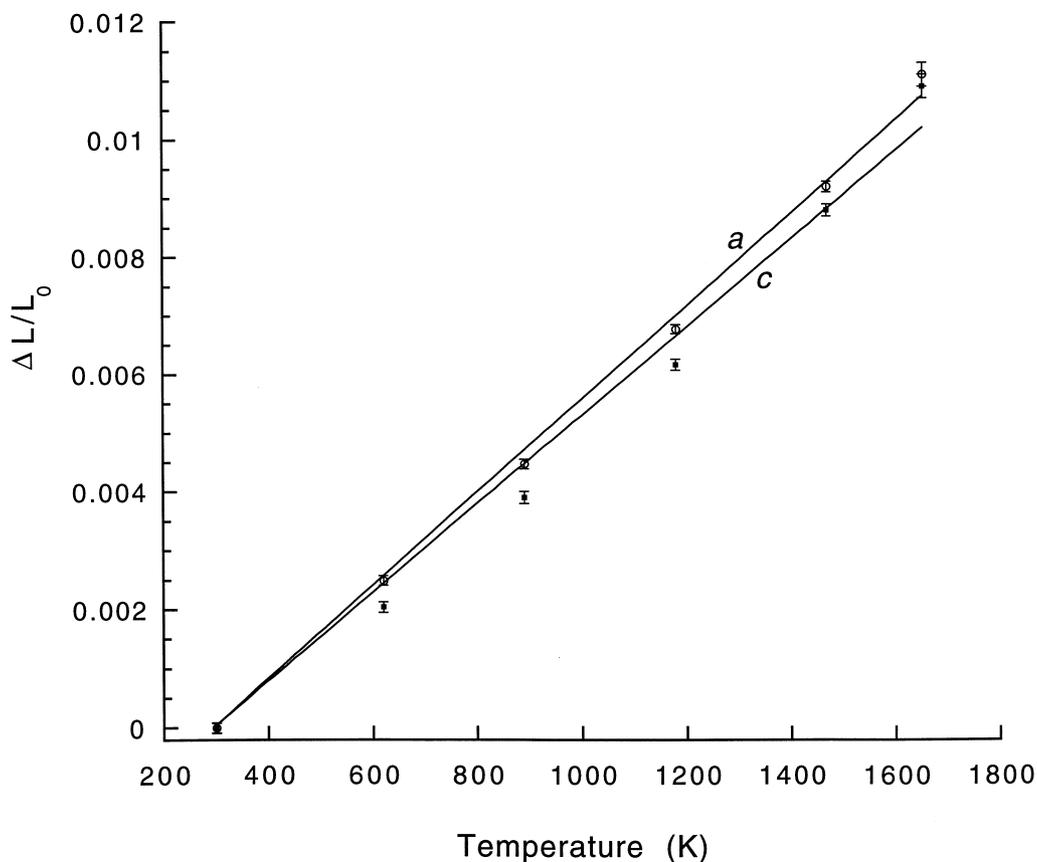


Fig. 5. Temperature dependence of $\Delta L/L_0$ for Mo_5SiB_2 .

Table 6
Mean CTE values and anisotropy determined in the temperature range specified in column 1

Temperature range (K)	$\bar{\alpha}_a$ (10^{-6} K $^{-1}$)	$\bar{\alpha}_c$ (10^{-6} K $^{-1}$)	$\bar{\alpha}_v$ (10^{-6} K $^{-1}$)	$\bar{\alpha}_c/\bar{\alpha}_a$
300–620	7.8(3)	6.4(3)	6.5(2)	0.8
620–890	7.3(3)	6.8(4)	7.1(3)	0.9
890–1179	7.9(3)	7.8(3)	7.9(3)	1.0
1179–1468	8.3(3)	9.0(3)	8.6(3)	1.1
1468–1652	10.0(9)	11(1)	10.4(9)	1.1

is the lattice parameter at 300 K. Using a linear fit, that has been constrained to zero expansion at 293 K, the slopes of the lines are $(7.9\pm 0.1)\times 10^{-6}$ K $^{-1}$ for a and $(7.5\pm 0.2)\times 10^{-6}$ K $^{-1}$ for c , where the number in parenthesis is one estimated standard deviation. The overall thermal expansion anisotropy is low and agrees well with Fu and Wang's [25] calculations. The lattice parameters of the Al₂O₃, present as a secondary phase, were also refined and agree well with the $\Delta L/L_0$ values calculated from the recommended equations to describe the thermal expansion of polycrystalline Al₂O₃ [26].

Table 6 gives the mean linear thermal expansion coefficients determined by:

$$\bar{\alpha} = \frac{\Delta L}{L_{\text{ave}}} \cdot \frac{1}{\Delta T} \quad (1)$$

where $L_{\text{ave}} = (L_{T1} + L_{T2})/2$ is the average lattice parameter in the temperature range $[T_1, T_2]$, $\Delta L = L_{T2} - L_{T1}$, and $\Delta T = T_2 - T_1$. Examination of Table 6 indicates that below 1000 K the mean coefficient of linear thermal expansion for a is greater than that of c . Near 1000 K $\bar{\alpha}_a$ and $\bar{\alpha}_c$ intersect, and above 1000 K the mean thermal expansion coefficient for c is greater than that of a . This means that the value of the thermal expansion anisotropy varies with temperature.

4. Conclusions

The room temperature structure determined in this study using neutron diffraction data collected on a polycrystalline sample of Mo₅SiB₂ made with boron enriched in ¹¹B agreed well with earlier results by Aronsson [19]. Mo₅SiB₂ crystallizes with a tetragonal unit cell, space group I4/mcm and with room temperature lattice parameters $a = 6.0272(3)$ and $c = 11.0671(7)$ Å. The structural refinements revealed that B substitutes for a minor amount of Si suggesting that the composition of T2 is not necessarily stoichiometric. The refined lattice parameters were studied as a function of temperature and the thermal expansion coefficients along the a and c -axes are, respectively, $(7.9\pm 0.1)\times 10^{-6}$ K $^{-1}$ and

$(7.5\pm 0.2)\times 10^{-6}$ K $^{-1}$. The low thermal expansion anisotropy is in contrast with that of Mo₅Si₃. The Si-Mo_{II} bond lengths which increase linearly with temperature over the entire temperature range, lie along the z axis while the B–B bonds, which increase linearly with temperature up to 1468 K and then change abruptly between 1468 and 1652 K, lie entirely in the xy plane. The fact that the lengths of different types of bonds increase differently with temperature is consistent with the observed change in the CTE anisotropy.

Acknowledgements

This research was sponsored by the Division of Materials Sciences, Office of Basic Energy Sciences and Engineering and by the Assistant Secretary for Energy Efficiency and Renewable Energy, Office of Transportation Technologies, as part of the High Temperature Materials Laboratory User Program, Oak Ridge National Laboratory. ORNL is managed by UT-Battelle, LLC, for the U.S. Department of Energy under contract number DE-AC05-00OR22725. CMH was supported in part by an appointment to the ORNL Postdoctoral Research Associates program jointly administered by ORAU and ORISE. The authors also thank Bryan Chakoumakos, ORNL, for assistance with the neutron powder diffraction data collection and processing, Larry Walker for the electron microprobe data, and Cecil Carmichael for the arc-melting.

References

- [1] Vasudevan AK, Petrovic JJ, Fishman SG, Sorrell CA, Nathal MV. Proceedings of the engineering foundation high temperature structural silicides conference, Hyannis, MA, USA. Materials Science and Engineering A 1999;A261:1.
- [2] Petrovic JJ, Vasudevan AK. Mater Sci Eng 1999;A261:1.
- [3] Sadananda K, Feng CR, Mitra R, Deevi SC. Mater Sci Eng 1999;A261:223.
- [4] Nowotny H, Dimakopoulou E, Kudielka H. Mh Chem 1957; 88:180.
- [5] Nunes CA, Sakidja R, Perepezko JH. In: Nathal, M.V. et al., editors. Structural intermetallics 1997, Warrendale, USA:TMS, 1997. p. 831.
- [6] Berczik DM. Method for enhancing the oxidation resistance of a molybdenum alloy, and a method of making a molybdenum alloy, 1997. United States Patent No. 5,595,616.
- [7] Berczik DM. Oxidation resistant molybdenum alloy, 1997. United States Patent No. 5,693,156.
- [8] Schneibel JH, Liu CT, Easton DS, Carmichael CA. Mater Sci Eng 1998;A261:78.
- [9] Meyer MK, Kramer MJ, Akinca [sic] M. Intermetallics 1996;4:273.
- [10] Chu F, Thomas DJ, McClellan K, Peralta P, He Y. Intermetallics 1997;7:611.
- [11] Fu CL, Wang X, Ye YY, Ho KM. Intermetallics 1999;7:179.
- [12] Schneibel JH. unpublished observation, 1997.
- [13] Thom AJ, Meyer MK, Kim Y, Akinc M. In: Ravi VA, Srivatsan TS, Moore JJ, editors. Processing and fabrication of advanced materials III. Warrendale, USA:TMS, 1994. p. 413.

- [14] Sakidja R, Sieber H, Perepezko JH, in: Crowson, A. et al., editors. *Molybdenum & molybdenum alloys*, Warrendale, USA:TMS, 1998. p. 99.
- [15] Sears VF. *Neutron News* 1992;3:26.
- [16] Yethiraj M, Fernandez-Baca JA. *Neutron scattering in materials science II*. MRS Symp Proc 1995;379:59.
- [17] Larson AC, Von Dreele RB. *General Structure Analysis System*. Los Alamos National Laboratory Report, 1994, LAUR 86-748.
- [18] Hewat AW. *Acta Cryst* 1979;A35:248.
- [19] Aronsson B. *Acta Chem Scand* 1958;12:31.
- [20] Ibers JA, Hamilton WC, editors. *International tables for X-ray crystallography, volume IV — revised and supplementary tables* to volumes II and III, The Kynoch Press, Birmingham, England, 1974, Tables 5.5A and 5.5B.
- [21] Sales BC, Chakoumakos BC, Mandrus D, Sharp JW. *J Solid State Chem* 1999;146:528.
- [22] Willis BTM, Pryor AW. *Thermal vibrations in crystallography*. London: Cambridge University Press, 1975.
- [23] Fu CL. Personal communication, 2000.
- [24] Kramer MJ. Unpublished data.
- [25] Fu CL, Wang X. *Phil Mag Let* 2000;80:683.
- [26] Touloukian YS, Ho CY, editors. *Thermophysical properties of matter; Vol 13. Thermal expansion of nonmetallic solids*. New York: IFI/Plenum, 1977.